Research Article

Seyed Morteza Naghib*, Yasser Zare, and Kyong Yop Rhee*

# A facile and simple approach to synthesis and characterization of methacrylated graphene oxide nanostructured polyaniline nanocomposites

https://doi.org/10.1515/ntrev-2020-0005
Received Nov 12, 2019; accepted Jan 7, 2020

**Abstract:** A novel, scalable methacrylated graphene oxide (MeGO) nanostructured polyaniline (PANI) nanocomposite was synthesized and electrodeposited on the surface of fluorine-doped tin oxide electrode (FTOE). The two-dimensional support maintained a suitable substrate and arrayed in a conductive polymer matrix, creating an ultra-superconductive platform with extraordinary characteristics. The versatility of the nanocomposite performance was corroborated by altering the amount of MeGO coated on FTOE and changing the charge density of electro-polymerized PANI on the substrate. This exceptional nanostructure material enabled a robust platform design that demonstrated the extraordinary performance with enhanced conductivity and stability. Charge transfer resistance ($R_{ct}$) was dramatically decreased from 11,000 $\Omega$ (for bare FTOE) to 65 $\Omega$ (for MeGO/PANI).

**Keywords:** Methacrylated graphene oxide; polyaniline; conducting polymers; electrochemical polymerization

## 1 Introduction

Since the industrialization of synthetic polymers, the polymers possessed sensitive attention in various applications [1, 2, 4–11]. For numerous years, there had been a vital requirement for a solid material, which could concurrently afford both processing features of polymers and exceptional electrical properties of metals [12]. Conductive polymers have been used in many applications due to their great sensibility, fast response time, ability to be used at ambient temperatures and low processing costs [13, 14]. Among them polyaniline [15, 16], polypyrrole [17] and polythiophene [18] have been considerably developed, due to their enhanced and unique characteristics. These include good conductivity toward electric current and ability to change their respective physical and chemical properties in response to an electrical stimulation [19]. Polyaniline is a promising member of conductive polymers family and has received great attention, due to its intriguing properties such as environmental stability, high conductivity, inexpensive starting material, unique redox process, facile synthesis, tunable properties, appropriate electrochemical and environmental stability, low cost, and strong bimolecular interactions [15, 16]. Nevertheless, the challenge remains to develop polymeric based nanocomposites that are amenable to the development of devices with broad conductivity and sensitivity [20–22].

Graphene and its derivatives are single layer sheets consisting carbon atoms [23], with $SP^2$ chemical bonds [4] forming a 2-D honeycomb crystal with precise atomic level organization [24, 25]. Exceptional characteristics of graphene make an advanced material for several interesting applications such as facile processability, fast production in comparison with other nanoscale carbons [26] and brilliant properties including exceptionally wide porosity, zero band gap [27], superior mobility of charge carriers (200,000 $cm^2v^{-1}s^{-1}$) [28], very high specific surface area (2630 $m^2g^{-1}$), great flexibility [29], unique chemical stability [30], fast electron transfer, prominent conductivity and cost efficiency [31, 32]. Due to superior features of graphene and its derivatives [33], some of them have remarkable attention comprising its exploitation as a functional substrate for prevention of nanoscale materials from aggregation and agglomeration [34] in catalysts [35], as a superb conductor in electrical devices and nanobiosensors, bio-acceptors in electrochemical sensing applications [36] and carriers [37] in drug delivery [38, 39].

***Corresponding Author: Seyed Morteza Naghib:** Nanotechnology Department, School of Advanced Technologies, Iran University of Science and Technology (IUST), P.O. Box 16846-13114, Tehran, Iran; Email: naghib@iust.ac.ir
***Corresponding Author: Kyong Yop Rhee:** Department of Mechanical Engineering, College of Engineering, Kyung Hee University, Yongin 446-701, Republic of Korea; Email: rheeky@khu.ac.kr
**Yasser Zare:** Department of Mechanical Engineering, College of Engineering, Kyung Hee University, Yongin 446-701, Republic of Korea

Recently, combining the carbon nanostructures with conductive polymers has attracted much attention. Among them, graphene-grafted PANI nanocomposites have been remarkably significant because of the excellent characteristics of 2D graphene nanosheets and good porosity of nanostructured PANI [40]. This strategy triggers outstanding sensitivity, improved conductivity, more selectivity and high capacity [41]. PANI and graphene possess $\pi$-conjugated electrons [30], that is why graphene is able to act as a nucleation center for the matrix, PANI, between the sheets of graphene. Therefore, they likewise establish excellent electron transfer from a reaction [42]. Consequently, improved mechanical strength and electrical conductivity are the main properties that can be expected [43] between graphene nanosheets with exceptional mechanical properties and PANI with high pseudocapacitance [44]. Many studies reported that graphene-grafted PANI composites are able to be utilized as electrode substrates. Recently, graphene/PANI composites, that have excellent electrochemistry and conductivity, are being used in several products such as nanobiosensors [45], electrochemical devices, energy storage equipment [46], etc. Recently, we have synthesized and fully characterized a graphene-grafted PANI composite as well as we developed and applied it for ascorbic acid and cancer detections. Here, we applied a new functionalization for developing graphene-grafted PANI composite.

The studies in the literature used conventional electrodes (*e.g.* gold and platinum), which are costly and less available. Also the modification of them is expensive and time consuming. In the present research, a simple electrode was used, which can be further amended with the nanocomposite film to increase conductivity. It is also possible to design a disposable sensor according to the structure and cost of FTOE. In summary graphene was functionalized in two stages. Then, the graphene was functionalized with a simple protocol using a low-cost method in the shortest time possible. Finally, PANI synthesized via electro-polymerization has been deposited on the obtained electrode. To the best of our knowledge, the nanocomposite consisting of MeGO and electropolymerized PANI was synthesized for the first time by a novel, simple and cost effective protocol, which can be applied in electrochemical biosensors, cardiac tissue engineering, biofuel cells and super-capacitors due to its extraordinarily high conductivity which can further increase sensitivity.

# 2 Experimental

## 2.1 Materials and solutions

Graphite fine powder (spectroscopic grade, particle size ≤ 50 μm), $NaNO_3$, $AgNO_3$, $KNO_3$, $H_2SO_4$, $KMnO_4$ and Potassium ferricyanide ($K_3Fe(CN)_6$) were obtained from Merck. 1-Ethyl-3-(3 dimethylaminopropyl) carbodiimide hydrochloride (EDC), N-hydroxysuccinimide (NHS), Phosphate-buffered saline (PBS), Dimethylformamide (DMF) and aniline (99%) were purchased from Sigma-Aldrich.

## 2.2 Preparation of the functionalized graphene, MeGO

Graphite oxide was prepared with the approach, modified Hummer [17]. Then, functionalized MeGO nanosheets were synthesized based on our previous study [20].

## 2.3 FTO modification by MeGO

For fabrication of modified electrode, FTO glass plates (8 $\Omega$ resistance) with the surface area of 0.25 $cm^2$, were prepared and sequential ultrasonic cleaning performed for 10 min in acetone, ethanol, isopropanol and deionized (DI) water, and then FTO sheets were dried under Ar gas flow. Then, MeGO suspended in DI was deposited (20, 30 and 40 μL) on the FTO surface by the cast coating method and it was allowed to dry at 45°C and the optimum volume was selected (40 μL).

## 2.4 Electro-polymerization of aniline

For electro-deposition of PANI on FTO modified with MeGO, 20 successive cyclic voltammograms in a solution consisting of 0.03 M aniline monomer and 0.5 M $H_2SO_4$ were applied on the electrode surface. This process was performed at the potential range of –0.4 to 1.2 and with the scan rate of 30 mV $s^{-1}$ [47].

## 2.5 Characterization

The Fourier transform infrared (FTIR) spectra were recorded in the range of 400-4500 $cm^{-1}$ with Shimadzu FTIR-8400s spectrometer (SHIMADZU-8400S, Japan). In order to study nanocomposite surface morphology, FE-

SEM images, EDX and mapping analysis were taken by Carl Zeiss FESEM instrument model Sigma. All electrochemical studies were performed using a Potentiostat/Galvanostat model of Autolab PGSTAT 30 (Echo chemie, B. V., Netherlands). The software of this device was Nova version 1.7.8. CV curves were obtained in the potential range of −0.8 to 0.8 V with the scan rate of 100 mV $s^{-1}$. Electrochemical impedance spectroscopy (EIS) measurements were accomplished in the frequency range of $10^{-1}$ – $10^{5}$ Hz, and the potential amplitude was 14 mV around the open circuit potential ($E_{ocp}$ = 0.22 V).

# 3 Results and discussion

## 3.1 Electro-polymerization of aniline

Aniline electro-polymerization was shown in Figure 1. As it can be seen, three redox peaks are observed, where the first (a and a′) is related to formation of cation-radicals and the second (b and b′) is due to production of by-products and intermediates. The last peaks (c and c′) are related to the formation of polymer chain propagation [48].

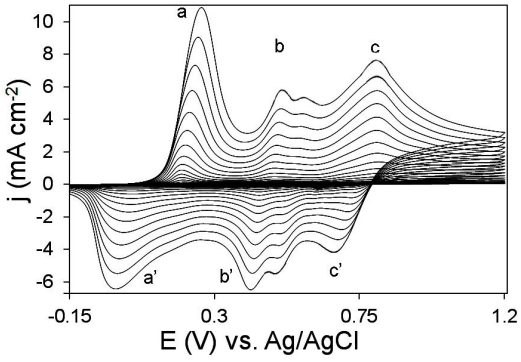


**Figure 1:** Electro-polymerization of aniline in 0.5 M $H_2SO_4$ containing 0.03 M aniline monomer (scan rate: 30 mV $s^{-1}$)

## 3.2 FT-IR analysis

Figure 2 shows the FT-IR spectra at different steps of the graphene functionalizing. In the spectrum of graphene oxide, corresponding peaks of 1054 and 1224 and 1620 $cm^{-1}$ are related to epoxide (COC) and C=O stretching vibration of ether and benzene ring, respectively. Peaks of 1050, 1617 and 1720 $cm^{-1}$ are attributed to acidic C-O, C=C (benzene ring) and C=O, respectively. They represent which represents the second stage of graphene oxide functionalization. The lack of epoxide ring peak proves that graphene oxide has been reduced to graphene. In the case of PANI peaks appeared in 3200-3600, 1450 and 1750 $cm^{-1}$ are related to N-H bond, and C=C (PANI benzene ring). Peak in 1200 $cm^{-1}$ indicates C=O bond in functionalized graphene. Spectrum peaks of PANI and MeGO/PANI exhibits some noise, because the diffuse reflectance spectroscopy (DRS) techniques have been applied to surface spectroscopy.

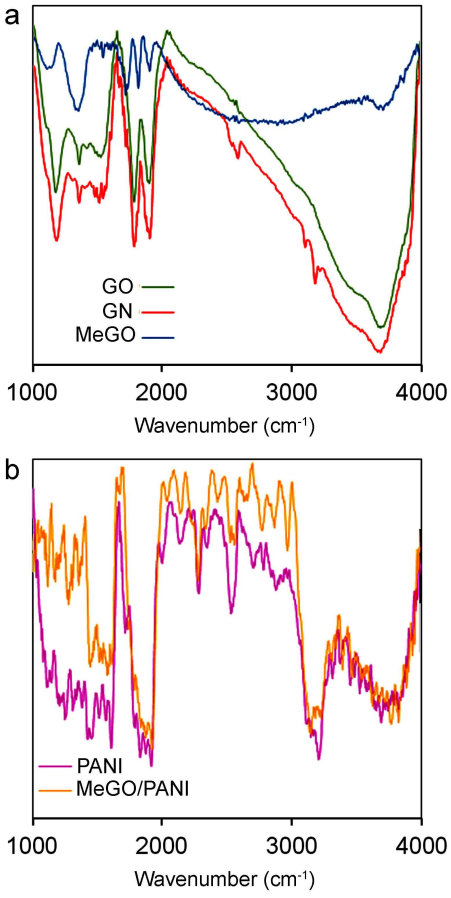


**Figure 2:** FT-IR spectrum of A) graphene oxide (GO), functionalized graphene with NHS/EDC (GN); MeGO and B) PANI, and MeGO/PANI

## 3.3 Microstructure analysis

FESEM analysis was performed to investigate the surface morphology of the nanocomposite and was shown in Figure 3. Graphene nanosheets can be seen in Figure 3a, where graphene nanosheets surface uniformity has changed after its modification with PANI (Figure 3b). It clearly shows that PANI is flattened on the surface and a porous structure is established.

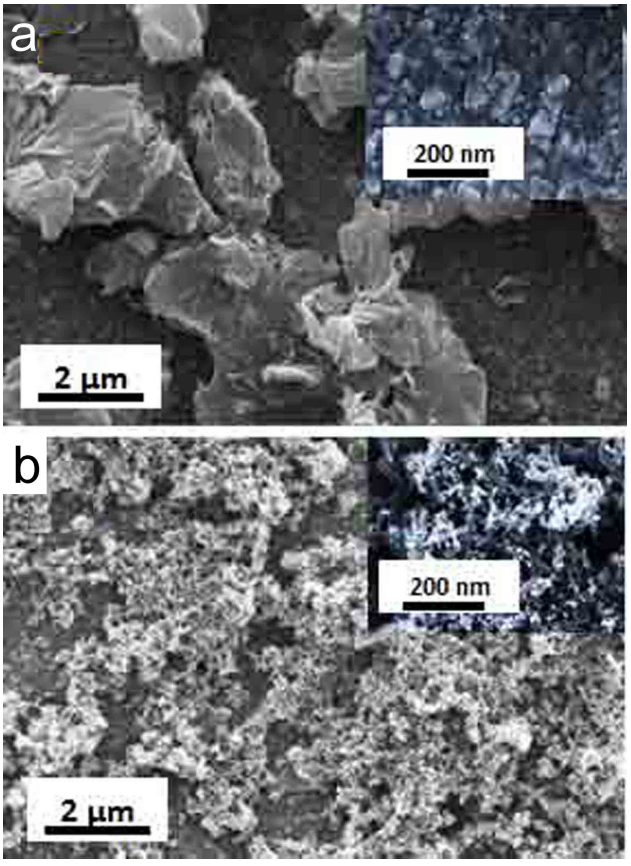


**Figure 3:** FESEM image analyses of a, d) MeGO; b, e) MeGO/PANI

## 3.4 Electrochemical investigations by cyclic voltammetry and EIS

For electrochemical investigations cyclic voltammetry and EIS techniques were used. For this study cyclic voltammograms in 0.01 M PBS (pH 7.4) containing 5 mM $K_3Fe(CN)_6$ were applied on FTO electrode, GO, MeGO, PANI, and MeGO/PANI. Also in another study, for each electrode Nyquist plots were obtained. The results of this experiment are illustrated in Figures 4 and 5 and Table 1 summarizes some important parameters extracted from these figures. These results indicate that, by modifying the electrode conductivity using surface treatment, resistance considerably decreases and the charge transfer resistance ($R_{ct}$) losses. In Nyquist diagram, the semicircle portion observed at high frequencies corresponds to $R_{ct}$.

This resistance can directly be measured as the semicircle diameter. In Figure 4A, a linear part can be seen at low frequencies due to limited mass transfer. This part in Figure 5A is negligible that can be concluded with modifying the electrode surface and increasing the conductivity, upon arrival of $Fe(CN)_6^{3-}$ probe to electrode surface, electron transfer occurs with high speed and due to diffusion

**Table 1:** Important parameters of modifying FTO electrode step by step

| Working electrode | $J_{ox}$ (mA cm$^{-2}$) | $R_s$ (Ω) | $R_{ct}$ (Ω) | $R_{ct}$ ME / $R_{ct}$ BE (%) |
|---|---|---|---|---|
| FTO | 0.38 | 95 | 11,000 | - |
| MeGO/PANI | 12.96 | 79 | 65 | 0.04 |

$J_{ox}$ – oxidation current density, $R_s$ – solution resistance, ME – modified electrode, BE – bare electrode

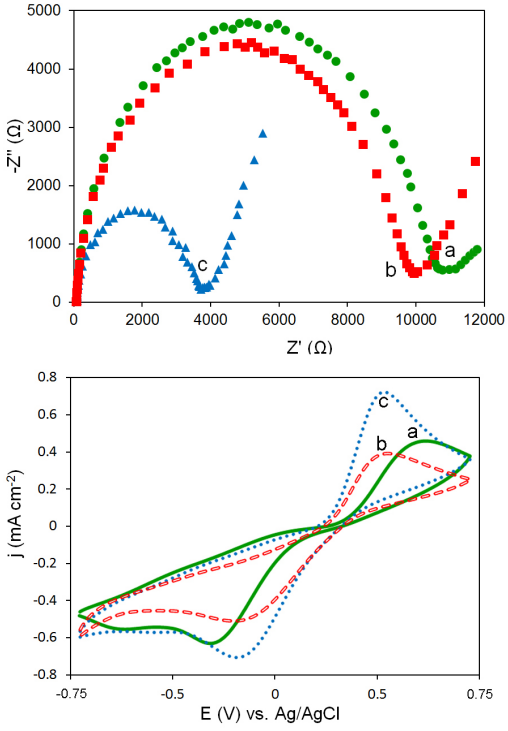


**Figure 4:** A and B: Nyquist plots and Cyclic voltammograms for a) FTO electrode, b) GO, and c) MeGO on the FTO surface in 5 mM $K_3Fe(CN)_6$ and 0.01 M PBS

layer formation and mass transfer limitation, linear part can be seen clearly.

According to Figures 4 and 5, there is a complete conformity between CV curves and Nyquist plots, because with decreasing the $R_{ct}$, peak height in CV increases and also, the highest charge transfer resistance ($R_{ct}$) is for bare FTO (~ 11,000 Ω) and at lowest (the best) is for the final modifying (MeGO/PANI) (~ 65 Ω), which is very lower than some previous reports. Table 2 is prepared for comparing this study with several researches. As can be seen in Table 2 $R_{ct}$ ME/ $R_{ct}$ BE or $R_{ct}$ PANI/ $R_{ct}$ BE in nanocomposite are lower than other recent studies. In MeGO/PANI, all components in modifying layer have synergistic effects by decreasing $R_{ct}$, increasing electrode conductivity and surface area.

**Table 2:** Comparing $R_{ct}$ of bare, PANI and modified electrode at this work with several recently published reports

| BE | ME | $R_{ct}$ of BE (Ω) | $R_{ct}$ of ME (Ω) | $R_{ct}$ of PANI (Ω) | $R_{ct}$ ME / $R_{ct}$ BE (%) | $R_{ct}$ ME / $R_{ct}$ PANI (%) | Reference |
|---|---|---|---|---|---|---|---|
| GCE | GR/PANI | 4,000 | 400 | - | 10.00 | - | [49] |
| Pt | GNS/MWCNT/PANI | 1.48 | 0.38 | 5.4 | 25.67 | 7.04 | [50] |
| Pt | PANI/8 wt% graphene | - | 11.49 | 64.5 | - | 17.81 | [51] |
| GCE | GR/PANI | 4,000 | 60 | - | 1.50 | - | [52] |
| GCE | ERGNO/PAN | 647 | 275 | 346 | 42.50 | 53.48 | [53] |
| ITO | GrO/PANI | - | 5,432 | 38,380 | - | 14.15 | [54] |
| GCE | PANIw/graphene | 800 | 20 | - | 2.5 | - | [55] |
| **FTO** | **MeGO/PANI** | **11,000** | **65** | **290** | **0.04** | **2.07** | **This work** |

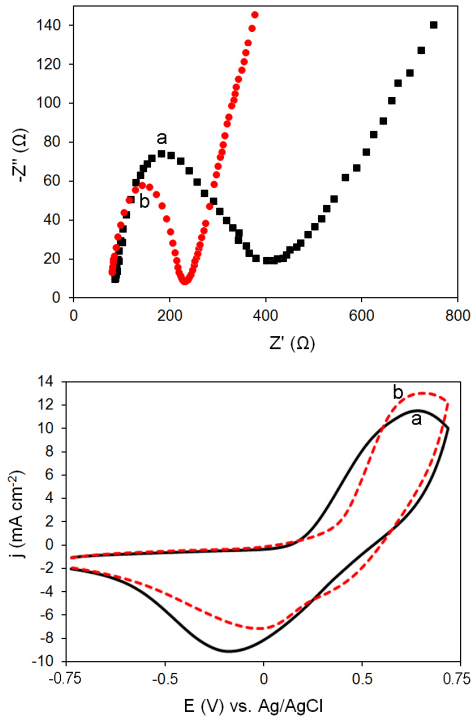


**Figure 5:** A and B: Nyqust plots and Cyclic voltammograms for a) PANI, and b) MeGO/PANI on the FTO surface in 5 mM K3Fe(CN)6 and 0.01 M PBS

In another experiment the stability of PANI, and MeGO/PANI on the FTO surface in 0.01 M PBS containing 5 mM $K_3Fe(CN)_6$ was studied by applying successive CVs (Figure 6). As the Figure shows, when only PANI is used for FTO modification, the stability of electrode response is relatively poor, due to the gradual dissolution of PANI in aqueous medium that would reduce the redox activity. In the case when MeGO is deposited on the electrode surface the stability is very good, and when a composite of both (MeGO/PANI) is used on the electrode surface, stability is considerably better than PANI alone. These results

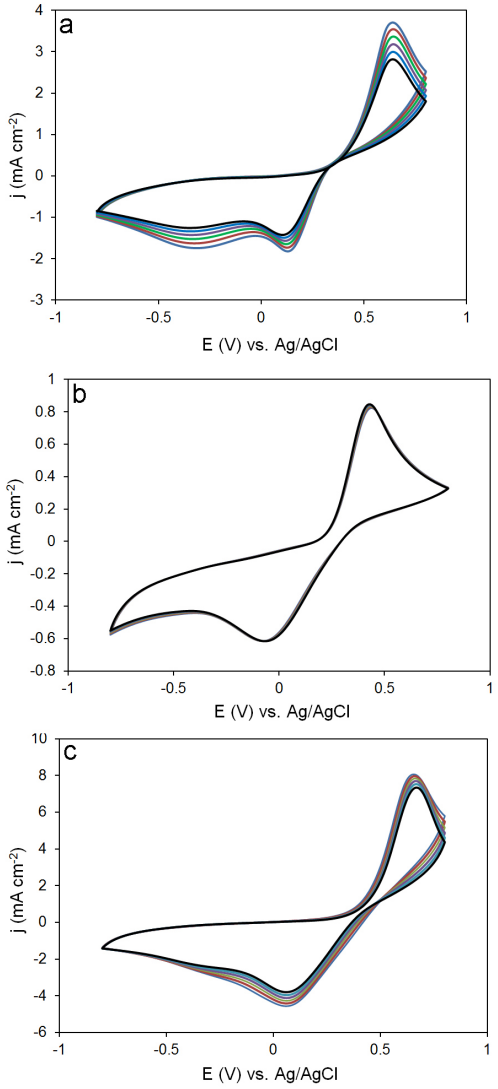


**Figure 6:** Cyclic voltammograms with 6 cycle for A: PANI, B: MeGO and C: MeGO/PANI on the FTO surface in 5 mM $K_3Fe(CN)_6$ and 0.01 M PBS

mean that the presence of MeGO improved PANI conductivity in water remarkably. Therefore, it also increases the electrochemical stability, that can be due to stronger interaction between benzene ring and graphene sheets and groups. These tests show an excellent electrochemical stability and repeatability in a neutral solution that is very important for practical applications in biosensors [56].

# 4 Conclusions

At first, graphene was functionalized in two stages using a low-cost method in a short time. Then, PANI was electropolymerized on MeGO nanosheets-based electrode that a layer by layer nanocomposite was formed. The results achieved by the experimental and theoretical data showed that MeGO/PANI nanocomposite can act as a successful nanomaterial for electrochemical biosensors, cardiac tissue engineering, biofuel cells and super-capacitors because of its excellent conductivity, which will increase its sensitivity. In future work, the nanocomposite will be used to construct a highly sensitive biosensor for ascorbic acid diagnosis and characterization.

**Acknowledgement:** The authors gratefully acknowledge the support of this work by the research councils of Iran University of Science and Technology (IUST).

# References

[1] Zare Y., Park S.P., Rhee K.Y., Analysis of complex viscosity and shear thinning behavior in poly (lactic acid)/poly (ethylene oxide)/carbon nanotubes biosensor based on Carreau–Yasuda model, Res. Phys., 2019, 13, 102245.

[2] Zhang P., Yi W., Xu H., Gao C., Hou J., Jin W., Lei Y., Hou X., Supramolecular interactions of poly with single-walled carbon nanotubes, Nanotechnol. Rev., 2018, 7(6), 487-495.

[3] Zare Y., Rhee K.Y., The effective conductivity of polymer carbon nanotubes (CNT) nanocomposites, J. Phys. Chem. Solids, 2019, 131, 15-21.

[4] Salahandish R., Ghaffarinejad A., Naghib S.M., Majidzadeh-A K., Sanati-Nezhad A., A novel graphene-grafted gold nanoparticles composite for highly sensitive electrochemical biosensing, IEEE Sens. J., 2018, 18, 2513-2519.

[5] Naghib S.M., Rabiee M., Omidinia E., Electroanalytical validation of a novel nanobiosensing strategy and direct electrochemistry of phenylalanine dehydrogenase for clinical diagnostic applications, Int. J. Electrochem. Sci, 2014, 9, 2301-2315.

[6] Roy S., Petrova R.S., Mitra S., Effect of carbon nanotube (CNT) functionalization in epoxy-CNT composites, Nanotechnol. Rev., 2018, 7, 475-485.

[7] Zare Y., Rhee K.Y., Expression of normal stress difference and relaxation modulus for ternary nanocomposites containing biodegradable polymers and carbon nanotubes by storage and loss modulus data, Compos. Part B: Eng., 2019, 158, 162-168.

[8] Zare Y., Rhim S., Garmabi H., Rhee K.Y., A simple model for constant storage modulus of poly (lactic acid)/poly (ethylene oxide)/carbon nanotubes nanocomposites at low frequencies assuming the properties of interphase regions and networks, J. Mech. Behav. Biomed. Mater., 2018, 80, 164-170.

[9] Zare Y., Rhee K., Evaluation and Development of Expanded Equations Based on Takayanagi Model for Tensile Modulus of Polymer Nanocomposites Assuming the Formation of Percolating Networks, Phys. Mesomech., 2018, 21, 351-357.

[10] Zare Y., Rhee K.Y., Modeling of viscosity and complex modulus for poly (lactic acid)/poly (ethylene oxide)/carbon nanotubes nanocomposites assuming yield stress and network breaking time, Compos. Part B: Eng., 2019, 156, 100-107.

[11] Kim S., Zare Y., Garmabi H., Rhee K.Y., Variations of tunneling properties in poly (lactic acid)(PLA)/poly (ethylene oxide)(PEO)/carbon nanotubes (CNT) nanocomposites during hydrolytic degradation, Sens. Actuat. A: Phys., 2018, 274, 28-36.

[12] Razavi R., Zare Y., Rhee K.Y., The roles of interphase and filler dimensions in the properties of tunneling spaces between CNT in polymer nanocomposites, Polym. Compos., 2019, 40 (2), 801-810.

[13] Liu H., Li Q., Zhang S., Yin R., Liu X., He Y., Dai K., Shan C., Guo J., Liu C., Electrically conductive polymer composites for smart flexible strain sensors: a critical review, J.Mater. Chem. C, 2018, 6, 12121-12141.

[14] Amoabeng D., Velankar S.S., A review of conductive polymer composites filled with low melting point metal alloys, Polym. Eng. Sci., 2018, 58, 1010-1019.

[15] Salahandish R., Ghaffarinejad A., Naghib S.M., Majidzadeh-A K., Zargartalebi H., Sanati-Nezhad A., Nano-biosensor for highly sensitive detection of HER2 positive breast cancer, Biosens. Bioelectr., 2018, 117, 104-111.

[16] Salahandish R., Ghaffarinejad A., Naghib S.M., Niyazi A., Majidzadeh-A K., Janmaleki M., Sanati-Nezhad A., Sandwich-structured nanoparticles-grafted functionalized graphene based 3D nanocomposites for high-performance biosensors to detect ascorbic acid biomolecule, Sci. Rep., 2019, 9, 1226.

[17] Stejskal J., Trchová M., Conducting polypyrrole nanotubes: a review, Chem. Papers, 2018, 72, 1563-1595.

[18] Chen Q., Wang X., Chen F., Zhang N., Ma M., Extremely strong and tough polythiophene composite for flexible electronics, Chem. Eng. J., 2019, 368, 933-940.

[19] Moon J.-M., Thapliyal N., Hussain K.K., Goyal R.N., Shim Y.-B., Conducting polymer-based electrochemical biosensors for neurotransmitters: A review, Biosens. Bioelectr., 2018, 102, 540-552.

[20] Naghib S.M., Two-dimensional functionalised methacrylated graphene oxide nanosheets as simple and inexpensive electrodes for biosensing applications, Micro & Nano Lett., 2019, 14, 462-465.

[21] Naghib S.M., Rahmanian M., Keivan M.A., Asiaei S., Vahidi O., Novel magnetic nanocomposites comprising reduced graphene oxide/Fe3O4/gelatin utilized in ultrasensitive non-enzymatic biosensing, Int. J. Electrochem. Sci, 2016, 11, 10256-10269.

[22] Omidinia E., Naghib S.M., Boughdachi A., Khoshkenar P., Mills D.K., Hybridization of silver nanoparticles and reduced graphene nanosheets into a nanocomposite for highly sensitive

L-phenylalanine biosensing, Int. J. Electrochem. Sci, 2015, 10, 6833-6843.
[23] Askari E., Naghib S.M., A novel approach to facile synthesis and biosensing of the protein-regulated graphene, Int. J. Electrochem. Sci, 2018, 13, 886-897.
[24] Naghib S.M., Parnian E., Keshvari H., Omidinia E., Eshghan-Malek M., Synthesis, characterization and electrochemical evaluation of polyvinylalchol/graphene oxide/silver nanocomposites for glucose biosensing application, Int. J. Electrochem. Sci, 2018, 13, 1013-1026.
[25] Kalkhoran A.H.Z., Naghib S.M., Vahidi O., Rahmanian M., Synthesis and characterization of graphene-grafted gelatin nanocomposite hydrogels as emerging drug delivery systems, Biomed. Phys. Eng. Expr., 2018, 4, 055017.
[26] Qu L., Liu Y., Baek J.-B., Dai L., Nitrogen-doped graphene as efficient metal-free electrocatalyst for oxygen reduction in fuel cells, ACS Nano, 2010, 4, 1321-1326.
[27] Mattevi C., Eda G., Agnoli S., Miller S., Mkhoyan K.A., Celik O., Mastrogiovanni D., Granozzi G., Garfunkel E., Chhowalla M., Evolution of electrical, chemical, and structural properties of transparent and conducting chemically derived graphene thin films, Adv. Funct. Mater., 2009, 19, 2577-2583.
[28] Zhu Y., Murali S., Cai W., Li X., Suk J.W., Potts J.R., Ruoff R.S., Graphene and graphene oxide: synthesis, properties, and applications, Adv. Mater., 2010, 22, 3906-3924.
[29] Yao Y., Miao S., Liu S., Ma L.P., Sun H., Wang S., Synthesis, characterization, and adsorption properties of magnetic Fe3O4 graphene nanocomposite, Chem. Eng. J., 2012, 184, 326-332.
[30] Wu Z., Chen X., Zhu S., Zhou Z., Yao Y., Quan W., Liu B., Enhanced sensitivity of ammonia sensor using graphene/polyaniline nanocomposite, Sens. Actuat. B: Chem., 2013, 178, 485-493.
[31] Chen F., Jia D., Jin X., Cao Y., Liu A., A general method for the synthesis of graphene oxide-metal sulfide composites with improved photocatalytic activities, Dyes and Pigments, 2016, 125, 142-150.
[32] Naghib S.M., Fabrication of Nafion/Silver Nanoparticles/Reduced Graphene Nanosheets/Glucose Oxidase Nanobiocomposite for Electrochemical Glucose Biosensing, Analyt. Bioanalyt. Electrochem., 2016, 8, 453-465.
[33] Kalkhoran A.H.Z., Vahidi O., Naghib S.M., A new mathematical approach to predict the actual drug release from hydrogels, Europ. J. Pharmaceut. Sci., 2018, 111, 303-310.
[34] Nag S., Roychowdhury A., Das D., Mukherjee S., Synthesis of $\alpha$-Fe2O3-functionalised graphene oxide nanocomposite by a facile low temperature method and study of its magnetic and hyperfine properties, Mater. Res. Bull., 2016, 74, 109-116.
[35] Ruecha N., Rangkupan R., Rodthongkum N., Chailapakul O., Novel paper-based cholesterol biosensor using graphene/polyvinylpyrrolidone/polyaniline nanocomposite, Biosens. Bioelectr., 2014, 52, 13-19.
[36] Sun L., Wang H., Eid K., Alshehri S.M., Malgras V., Yamauchi Y., Wang L., One-Step Synthesis of Dendritic Bimetallic PtPd Nanoparticles on Reduced Graphene Oxide and Its Electrocatalytic Properties, Electrochimica Acta, 2016, 188, 845-851.
[37] Gooneh-Farahani S., Naghib S.M.N., Naimi-Jamal M.R., A Critical Comparison Study on the pH-Sensitive Nanocomposites Based on Graphene-Grafted Chitosan for Cancer Theragnosis, Multidisc. Cancer Investig., 2019, 3, 5-16.
[38] Askari E., Naghib S.M., Seyfoori A., Maleki A., Rahmanian M., Ultrasonic-Assisted Synthesis and In Vitro Biological Assessments of a Novel Herceptin-Stabilized Graphene Using Three Dimensional Cell Spheroid, Ultrason. Sonochem., 2019, 104615.
[39] Gooneh-Farahani S., Naimi-Jamal M.R., Naghib S.M., Stimuli-responsive graphene-incorporated multifunctional chitosan for drug delivery applications: a review, Expert Opinion on Drug Deliv., 2019, 16, 79-99.
[40] Hao Q., Wang H., Yang X., Lu L., Wang X., Morphology-controlled fabrication of sulfonated graphene/polyaniline nanocomposites by liquid/liquid interfacial polymerization and investigation of their electrochemical properties, Nano Res., 2011, 4, 323-333.
[41] Wang L., Lu X., Lei S., Song Y., Graphene-based polyaniline nanocomposites: preparation, properties and applications, J. Mater. Chem. A, 2014, 2, 4491-4509.
[42] Al-Mashat L., Shin K., Kalantar-Zadeh K., Plessis J.D., Han S.H., Kojima R.W., Kaner R.B., Li D., Gou X., Ippolito S.J., Graphene/polyaniline nanocomposite for hydrogen sensing, J. Phys. Chem. C, 2010, 114, 16168-16173.
[43] Kumar N.A., Choi H.-J., Shin Y.R., Chang D.W., Dai L., Baek J.-B., Polyaniline-grafted reduced graphene oxide for efficient electrochemical supercapacitors, ACS Nano, 2012, 6, 1715-1723.
[44] Gao Z., Yang W., Wang J., Yan H., Yao Y., Ma J., Wang B., Zhang M., Liu L., Electrochemical synthesis of layer-by-layer reduced graphene oxide sheets/polyaniline nanofibers composite and its electrochemical performance, Electrochimica Acta, 2013, 91, 185-194.
[45] Ameen S., Akhtar M.S., Shin H.S., Hydrazine chemical sensing by modified electrode based on in situ electrochemically synthesized polyaniline/graphene composite thin film, Sens. Actuat. B: Chem, 2012, 173, 177-183.
[46] Xia X., Hao Q., Lei W., Wang W., Wang H., Wang X., Reduced-graphene oxide/molybdenum oxide/polyaniline ternary composite for high energy density supercapacitors: Synthesis and properties, J. Mater. Chem., 2012, 22, 8314-8320.
[47] Darowicki K., Kawula J., Impedance characterization of the process of polyaniline first redox transformation after aniline electropolymerization, Electrochimica acta, 2004, 49, 4829-4839.
[48] Gvozdenović M.M., Grgur B.N., Jugović B.Z., Stevanović J.S., Trišović T.L., Electrochemical polymerization of aniline, 2011, INTECH Open Access Publ.
[49] Liu S., Xing X., Yu J., Lian W., Li J., Cui M., Huang J., A novel label-free electrochemical aptasensor based on graphene–polyaniline composite film for dopamine determination, Biosens. Bioelectr., 2012, 36, 186-191.
[50] Al-Bahrani M.R., Xu X., Ahmad W., Ren X., Su J., Cheng Z., Gao Y., Highly efficient dye-sensitized solar cell with GNS/MWCNT/PANI as a counter electrode, Mater. Res. Bulletin, 2014, 59, 272-277.
[51] He B., Tang Q., Wang M., Ma C., Yuan S., Complexation of polyaniline and graphene for efficient counter electrodes in dye-sensitized solar cells: Enhanced charge transfer ability, J. Power Sourc., 2014, 256, 8-13.
[52] Fan Y., Liu J.-H., Yang C.-P., Yu M., Liu P., Graphene–polyaniline composite film modified electrode for voltammetric determination of 4-aminophenol, Sens. Actuat. B: Chem., 2011, 157, 669-674.
[53] Du M., Yang T., Li X., Jiao K., Fabrication of DNA/graphene/polyaniline nanocomplex for label-free voltammetric detection of DNA hybridization, Talanta, 2012, 88, 439-444.
[54] Radhapyari K., Kotoky P., Das M.R., Khan R., Graphene–polyaniline nanocomposite based biosensor for detection of antimalarial drug artesunate in pharmaceutical formulation and

biological fluids, Talanta, 2013, 111, 47-53.
[55] Bo Y., Yang H., Hu Y., Yao T., Huang S., A novel electrochemical DNA biosensor based on graphene and polyaniline nanowires, Electrochimica Acta, 2011, 56, 2676-2681.
[56] Luo J., Jiang S., Liu R., Zhang Y., Liu X., Synthesis of water dispersible polyaniline/poly (styrenesulfonic acid) modified graphene composite and its electrochemical properties, Electrochimica Acta, 2013, 96, 103-109.